

# Low-impedance time-domain reflectometry for measuring the impedance characteristics of low-impedance transmission lines

N. G. Paulter<sup>a)</sup> and R. H. Palm

*Electricity Division, National Institute of Standards and Technology, Gaithersburg, Maryland 20899*

A. R. Hefner and D. W. Berning

*Semiconductor Electronics Division, National Institute of Standards and Technology, Gaithersburg, Maryland 20899*

(Received 10 June 2003; accepted 1 September 2003)

An experimental examination of a 10  $\Omega$  and a 2  $\Omega$  time-domain reflectometer (TDR) technique for measuring low-impedance transmission line characteristics is presented. TDR measurements using these systems are compared to those using a 50  $\Omega$  TDR system. The results show that the uncertainties in the characteristic impedance,  $Z_C$ , of a low- $Z_C$  transmission line are a significant fraction of  $Z_C$  for 50  $\Omega$  TDR measurements, whereas the fractional uncertainties are much less when using a low-impedance TDR. The fractional  $Z_C$  uncertainties for the 50  $\Omega$  TDR increase as  $Z_C$  decreases. [DOI: 10.1063/1.1622981]

## I. INTRODUCTION

Time-domain reflectometers (TDRs) are often used for determining the electrical properties of electronic and electrical circuits, such as the location of opens and shorts in circuits, the electromagnetic wave propagation characteristic (characteristic impedance, propagation function) of transmission lines, the magnitude and location of perturbations in transmission lines (reflection and transmission coefficients, impedance changes), the lumped circuit element parameters (resistance, capacitance, inductance, impulse response), the impedance profiles of populated and unpopulated circuits, etc. The application considered here is the determination of the characteristic impedance,  $Z_C$ , of low- $Z_C$  ( $< 30 \Omega$ ) transmission lines.

Electrical conductors and interconnects in a circuit behave as transmission lines when the electrical length of the conductor is approximately equal to or greater than the wavelengths of the highest propagating frequencies of the conducted signal. This situation is usually encountered in high-speed/high-frequency circuits. For this work, high-speed/high-frequency will refer to signals that have transition durations less than 350 ps or, equivalently, 3 dB attenuation bandwidths greater than 1 GHz.

A recent analysis<sup>1</sup> has shown that errors and measurement uncertainties may be significant when trying to determine the  $Z_C$  of low- $Z_C$  transmission lines or the magnitude of impedance discontinuities in low- $Z_C$  transmission lines with a 50  $\Omega$  TDR. These problems are even greater when  $Z_C$  is less than or equal to 10  $\Omega$ . Low- $Z_C$  transmission lines are now being used in certain high-speed memory buses ( $Z_C \approx 28 \Omega$ ) and in bus bars ( $Z_C \leq 28 \Omega$ ) used for high-power switching circuits, which may contain noise in the tens of megahertz range<sup>2-4</sup> that can radiate from impedance discontinuities.

The difficulty in developing a low-impedance TDR system is in efficiently launching the pulse onto the transmission line without degrading pulse properties (primarily bandwidth and amplitude) and in sampling that pulse without degrading pulse properties, lowering measurement system bandwidth, or introducing spurious components into the TDR waveform. Section II provides a brief background on TDR measurements. Section III contains a description of a low-impedance TDR, including its signal launch and probing substructures. In Secs. IV and V measurement results are presented.

## II. BACKGROUND

A TDR system is similar to a sampling oscilloscope except that the TDR head contains both a sampling device (the sampler) and a pulse generator. The generated or incident pulse is typically a rectangular pulse with a fast transition between its low-voltage state or base line (nominally 0 V) and its high-voltage state (nominally 0.20–0.25 V). The transition duration (rise time) of the pulses used in typical TDRs is usually less than 30 ps. The pulse duration, on the other hand, is very long, typically much longer than the epoch over which the TDR waveform is observed. Because the pulse duration is much longer than the waveform epoch, the TDR pulse effectively appears to be a step-like pulse (high state continues forever). Reflections are caused as the propagating pulse encounters impedance discontinuities along the transmission line (TL), as is shown in the example of Fig. 1. In Fig. 1, the TDR waveform corresponds to a continuous uniform lossless transmission line (of length  $\mathcal{L}$  and characteristic impedance  $Z_C$ ) that is connected to the TDR head at one end and unterminated (open circuit) at the other end. This TDR waveform is the result of the reflections occurring at the TDR/TL interface and at the TL/open-circuit interface; the reflected pulses add to the incident pulse. In Fig. 1, the levels labeled  $L_0$  and  $L_1$  are of the low and high states of the incident pulse. The amplitude of the pulse that is reflected

<sup>a)</sup>Author to whom correspondence should be addressed; electronic mail: nicholas.paulter@nist.gov

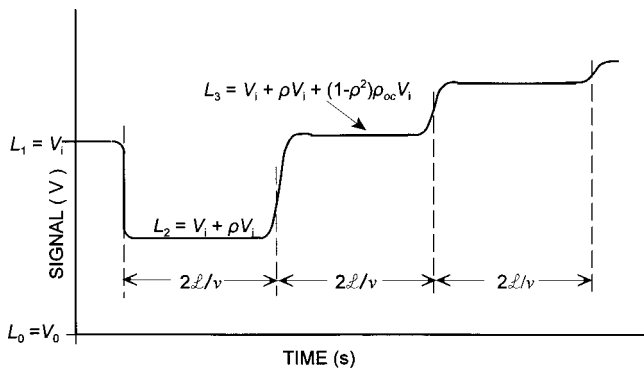


FIG. 1. An ideal TDR waveform for a uniform continuous transmission line of length  $L$  with an open circuit termination and with propagation velocity  $v$ .  $V_0$  and  $V_i$  are the base line and top line values of the incident pulse,  $\rho$  is the reflection coefficient from the transmission line, and  $\rho_{oc}$  is the open circuit reflection coefficient.

from the impedance discontinuity is dependent on the impedances on either side of the discontinuity. A good way of envisioning how and which pulses will add to create the TDR waveform is through the reflection-transmission (RT) diagram shown in Fig. 2. The level  $L_2$  in Fig. 1 is the result of the addition of the incident pulse and the first reflected pulse as indicated in Fig. 1 and diagrammatically by the top two leftward directed arrows in the RT diagram (Fig. 2). The level  $L_3$  is the result of the addition of the incident pulse, the first reflected pulse, and the second reflected pulse. The instants the reflections occur in the TDR waveform are dependent on the pulse propagation velocity in the transmission line and the separation between impedance discontinuities.

**III. LOW-IMPEDANCE TDR DESIGN**

The low-impedance TDR consists of the low characteristic impedance transmission line (which will be the reference impedance), a means of launching a signal (the pulse) from a  $50 \Omega$  source onto the reference transmission line

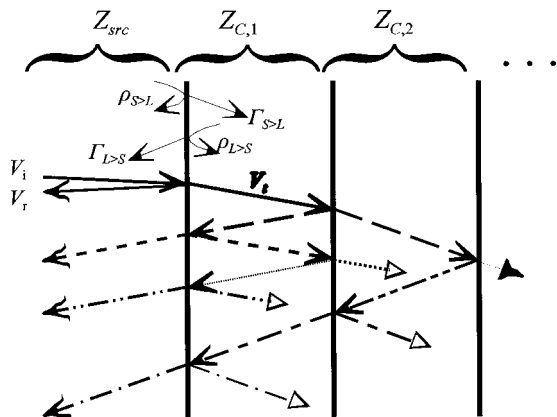


FIG. 2. The transmission/reflection diagram for a three-impedance system,  $Z_{src}$ ,  $Z_{C,1}$ , and  $Z_{C,2}$ , connected in series. The reflected and transmitted pulses associated with a given incident pulse at each interface are shown with similar line styles. The solid triangular arrow indicates the pulse has passed through the last interface and no longer adds information to the reflection (TDR) waveform. The hollow triangle arrows indicate the reflections associated with the last transmission may still contribute to the TDR waveform. The curly arrows at the left indicate the contributions to the TDR waveform.

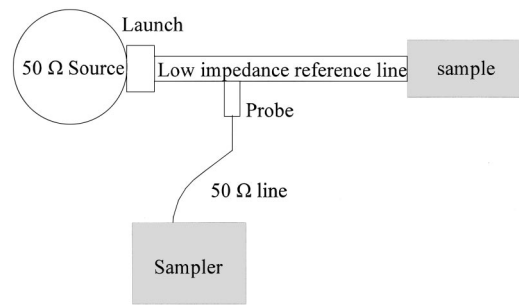


FIG. 3. Low-impedance test system.

(RTL), and a means of sampling the pulse as it propagates along the RTL (see Fig. 3). The transmission line sample is connected to the RTL as shown in Fig. 3. For the experiments described later, two reference lines were used, one having a characteristic impedance of  $10 \Omega$  and the other of  $2 \Omega$ .

**A. Transmission line**

The RTL used in the test system described herein is a parallel plate structure consisting of one ground line and one signal line. These lines are of equal width and are located on opposite sides of an insulator. The parallel plate transmission line (PPTL) was chosen because both ground and signal lines are directly accessible, therefore, no vias or holes are required to connect to the ground and signal conductors as would be the case for a stripline or coaxial structure. Furthermore, the models used to describe the electrical behavior of the PPTL are simple compared to those of other planar structures (microstrip, coplanar strips, or coplanar waveguide) and, for an ideal (uniform, lossless) line, have a closed form solution for  $Z_C$ .

**B. Launch design**

The launch has two electrical functions. One function is to provide efficient transmission of the incident pulse from the source to the reference transmission line. The launch must maintain the integrity of the propagating signal, that is, the amplitude and temporal characteristics of the signal should be minimally affected. For the purpose of this discussion, signal propagation from the source to the RTL is the forward direction and propagation from the RTL to the source is the backward direction. The other function of the launch is to minimize reflections from the RTL/source interface; these are reflections that will couple back into the TDR waveform. If we look at Fig. 2, these reflections are shown diagrammatically as those from the leftmost vertical line that travel to the right. These two requirements for the launch, preserving signal integrity and reducing RTL/source reflections, have opposing design requirements. Two different circuit designs were tested (see Fig. 4) for use as the launch.

The forward-matched design (fd) is the least flexible and trying to obtain a close match (within  $\pm 2 \Omega$ ) to the  $50 \Omega$  source is very difficult. The resistance value of  $R_1$  should ideally be  $40 \Omega$  for a  $Z_C = 10 \Omega$ . Furthermore, the fd only allows either maximization of the transmission through the source/RTL junction into the RTL or minimization of the

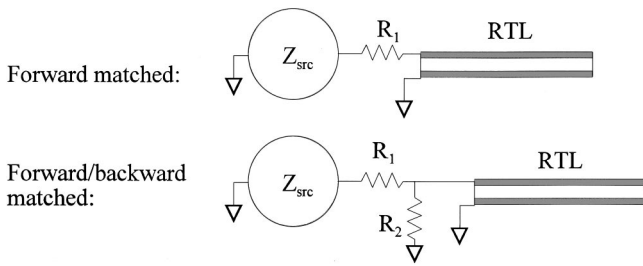


FIG. 4. Electrical diagram of the two launch designs considered. The RTL is shown in side view, with the upper gray region depicting the signal line and the lower gray region the ground plane.

reflections from the RTL/source interface back into the RTL. The forward/backward-matched design (f/bd), on the other hand, allows for optimization of both the forward transmission and backward reflection functions.

In this section, four different ways of characterizing launch performance are measured and analyzed. These four ways are:

- (1) Reflection coefficient of the launch for the forward direction, Sec. III B 1. This shows how well the launch is matched to the 50 Ω source.
- (2) Multiple reflections within the RTL, without the probe in contact, Sec. III B 2. This shows how well matched the RTL (which for this study is 10 Ω) is to the launch.
- (3) Multiple reflections within the RTL, with the probe in contact, Sec. III B 3. This shows how the probe adds additional reflections and how well those reflections are terminated by the launch.
- (4) TDR of the launch from the RTL perspective, Sec. III B 4. This shows the same information as item 3 but from the perspective of the RTL.

**1. Reflection coefficient of launch, forward direction**

This section describes signals that propagate up to the launch from the TDR, are reflected from the TDR/launch interface (TDR is acting as the source), and that are subsequently measured by the conventional 50 Ω TDR. These signals provide information on the launch efficiency. Ideally, the launch should appear as a 50 Ω load to the source (which, in this case, is the 50 Ω TDR). Figure 5 shows the reflection waveform for both the fd and the f/bd. The experimental arrangement is shown diagrammatically in the lower right of Fig. 5. In Fig. 5, the large oscillations between about  $3.5 \times 10^{-10}$  s and  $6 \times 10^{-10}$  s correspond to reflections from the TDR/RTL interface. The forward-going reflection coefficient,  $\rho_{S>L}$ , is given by the amplitude of the reflected signal divided by the amplitude of the incident signal

$$\rho_{S>L} = \frac{V_{\text{refl}}}{V_{\text{in}}}, \tag{1}$$

where  $V_{\text{refl}}$  is the reflected voltage and  $V_{\text{in}}$  is the incident voltage. For all the data given herein,  $V_{\text{in}} = 0.25$  V. For the fd curve shown in Fig. 5,  $V_{\text{fd,refl}} = 0.012$  V (0.015 V–0.003 V), which gives  $\rho_{\text{fd},S>L} = 0.05$ . Assuming that the impedance of

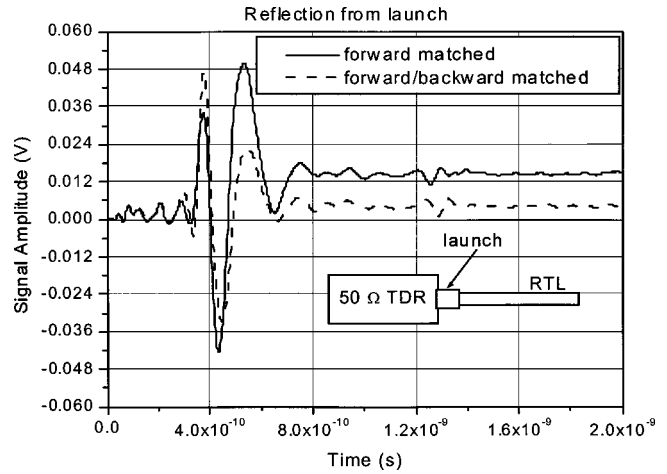


FIG. 5. TDR-measured reflection waveforms from launch end of transmission line. The experimental arrangement is shown diagrammatically in the lower right.

the TDR and RTL are 50 Ω and 10 Ω, respectively, the resistance value of the launch as seen by the TDR can be calculated from

$$Z_{\text{fd,C}} = \frac{1 + \rho}{1 - \rho} Z_{\text{src}} \tag{2}$$

and

$$Z_{\text{fd,C}} = R_1 + Z_C, \tag{3}$$

where  $Z_{\text{fd,C}}$  is the electrical load attached to the TDR source.  $R_1$  can be determined using Eqs. (2) and (3) with  $\rho = \rho_{\text{fd},S>L}$ . The value of  $R_1$  is calculated to be 45.3 Ω, which is close to the value expected for the two 91.9 Ω resistors used in parallel in the fd. The resistance values are those of available off-the-shelf chip resistors. This value of  $R_1$  is that measured at dc and also specified by the manufacturer. In an attempt to get  $R_1$  closer to 40 Ω, other combinations of commercially available resistance values were tested. However, use of more than two parallel resistors increased the magnitude of the oscillations seen at the RTL/source interface, probably due to increased capacitance, and are not considered here. Selecting  $R_1$  with a resistance value closer to the ideal value will reduce  $\rho_{\text{fd},S>L}$  (see Sec. III B 2). For the f/bd curve shown in Fig. 5,  $V_{\text{f/bd,refl}} = 0.0016$  V, which gives  $\rho_{\text{f/bd},S>L} = 0.006$ . For the f/bd case, the electrical load attached to the sampler is given by

$$Z_{\text{f/bd,C}} = R_1 + \left( \frac{1}{Z_C} + \frac{1}{R_2} \right)^{-1}. \tag{4}$$

The same value of  $R_1$  that was used in the fd is also used in the f/bd. Using  $R_1 = 45.3$  Ω,  $Z_{\text{src}} = 50$  Ω, and  $Z_C = 10$  Ω, and using Eq. (4) in Eq. (2), an estimate for  $R_2$  can be obtained;  $R_2 = 11.3$  Ω. This value of  $R_2$  is the same as the manufacturer specified and dc measured values of 11.3 Ω.  $R_2$  was an off-the-shelf resistor and selecting  $R_1$  and  $R_2$  with resistance values closer to the ideal values will reduce the magnitude of  $\rho_{\text{f/bd},S>L}$  (see Sec. III B 2). However, it is important to note, that even with off-the-shelf resistors, the f/bd yields a much smaller launch reflection coefficient than does the fd.

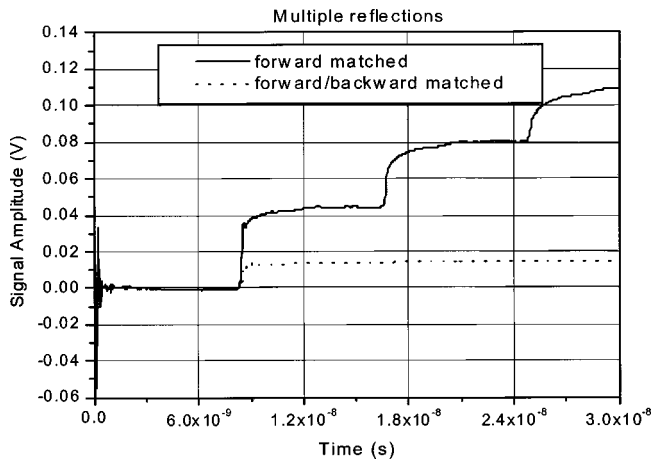


FIG. 6. TDR-measured reflection waveforms of the pulse reflected within the transmission line.

**2. Multiple reflections within the RTL, without probe in contact with the RTL**

This section provides information on the magnitude of the backward-going signals that are reflected from the launch/TDR interface and that are subsequently measured by the conventional 50 Ω TDR. Multiple reflections may be observed in the TDR waveform (refer to Fig. 2). Ideally, the signals incident on the launch/TDR from the launch side should not reflect back into the launch. Figure 6 shows the multiple reflections that occur within the RTL. The experimental arrangement is the same as that shown diagrammatically in the lower right of Fig. 5. The series of levels shown in Fig. 6 can be described by the following equation:

$$V_{\text{refl,obs}} = V_{\text{in}}(1 + \rho_{S>L} + \Gamma_{S>L}\Gamma_{L>S} + \Gamma_{S>L}\rho_{L>S}\Gamma_{L>S} + \Gamma_{S>L}\rho_{L>S}^2\Gamma_{L>S} + \dots) \quad (5)$$

In Eq. (5) and all subsequent analysis, it will be assumed that the reflection coefficient for the open end of the transmission line is 1.

The forward-going transmission coefficient for the fd,  $\Gamma_{\text{fd},S>L}$ , is given by

$$\Gamma_{\text{fd},S>L} = 1 - \rho_{\text{fd},S>L} \quad (6)$$

For the case given here,  $\Gamma_{\text{fd},S>L} = 0.95$ . The backward-going reflection coefficient,  $\rho_{\text{fd},L>S}$ , is given by

$$\rho_{\text{fd},L>S} = \frac{R_1 + Z_{\text{src}} - Z_C}{R_1 + Z_{\text{src}} + Z_C} \quad (7)$$

For the RTLs used here,  $\rho_{\text{fd},L>S} = 0.81$  and using this value in Eq. (6) gives  $\Gamma_{\text{fd},L>S} = 0.19$ . The curves shown in Fig. 6 have been offset (by subtracting 0.263 V, which is the value corresponding to  $V_{\text{in}}[1 + \rho_{S>L}]$ ) so that the first state level (leftmost level in Fig. 6) equals 0 V. Consequently, we calculate the state levels in the TDR waveform to be approximately: 0 V (corresponding to the reflection from the TDR/RTL interface), 0.045 V, 0.082 V, and 0.112 V. These values are what is approximately shown in Fig. 6 for the fd.

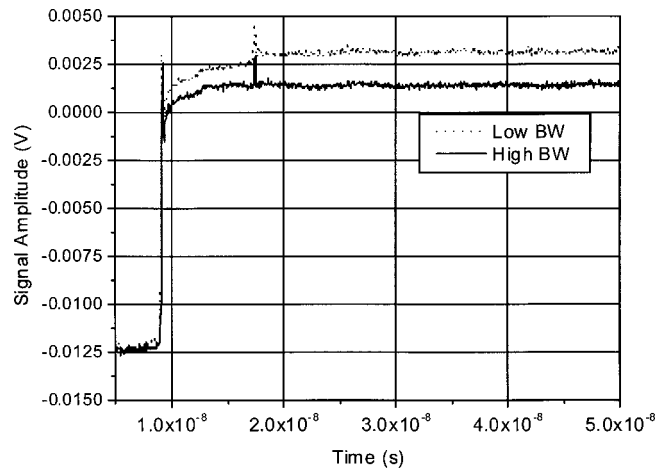


FIG. 7. TDR-measured reflection waveforms of the pulse reflected within the transmission line using off-the-shelf low bandwidth (Low BW) and custom high bandwidth (High BW) resistors.

The forward-going transmission coefficient for the f/bd,  $\Gamma_{\text{f/bd},S>L}$ , is a little more complicated to compute since some of the signal is shunted to ground via  $R_2$ . The  $\Gamma_{\text{f/bd},S>L}$  can be calculated using circuit analysis and is

$$\Gamma_{\text{f/bd},S>L} = (1 - \rho_{\text{f/bd},S>L}) \frac{R_2}{R_2 + Z_C} \quad (8)$$

For the value of  $R_2$  and  $Z_C$  used here,  $\Gamma_{\text{f/bd},S>L} = 0.527$ . The values of the backward-going reflection and transmission coefficients can be computed using the same methodology as done for the fd. Doing this gives  $\rho_{\text{f/bd},L>S} = 0.005$  and  $\Gamma_{\text{f/bd},L>S} = 0.105$ . Therefore, the expected TDR state levels after being offset (by subtraction of 0.252 V) are: 0 V, 0.014 V, and 0.014 V. Although these values do not match identically with those shown in Fig. 6, they do show close agreement. Moreover, it can be seen in Fig. 6 that voltage levels caused by multiple reflections have been effectively removed in the f/bd. More careful selection of the resistors reduces the magnitude of the reflection further, see Fig. 7. Figure 7 shows two traces of the backward-going pulse for the f/bd, one using off-the-shelf low bandwidth resistors (around 2 GHz) and the other using custom high bandwidth resistors (about 20 GHz). This figure shows several effects for the fb/d: (1) quicker settling of the TDR waveform after the major transition with the high bandwidth resistor, (2) flatter base line prior to the transition for the high bandwidth resistor, and (3) no observable level shift after the transient for the high bandwidth resistor.

It can be seen from the previous discussion that the launch of the f/bd produces significantly smaller reflections than the fd. Smaller reflections will produce smaller errors and uncertainties in the calculation of the impedance characteristics of the transmission line. For the 10 Ω transmission line and 50 Ω source impedance used in the discussion thus far, the values of  $R_1$  and  $R_2$  that will cause  $\rho_{\text{f/bd},S>L}$  and  $\rho_{\text{f/bd},L>S}$  to equal zero, the ideal situation, are  $R_1 = 44.72 \Omega$  and  $R_2 = 11.18 \Omega$ .



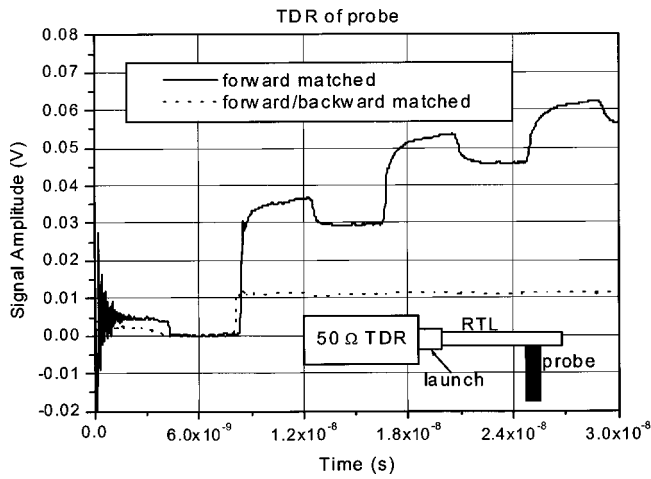


FIG. 8. TDR-measured reflection waveforms of the pulse reflected within the transmission line with the probe in place. The experimental arrangement is shown diagrammatically in the lower right.

**3. Multiple reflections within the RTL, with probe in contact with the RTL**

This section deals with signal perturbation caused by the probe. Ideally, the probe should not affect the propagating signal. The data are shown for signals acquired with a conventional TDR. As was done in Sec. III B 2, an analysis will be performed in this section to describe the state levels in TDR waveforms shown in Fig. 8. The experimental arrangement is shown diagrammatically in the lower right of Fig. 8. In addition to the reflections considered in Sec. III B 2, there will be other reflections from the location where the probe contacts the transmission line. The levels in the reflection waveform when the probe is in place are given by

$$V_{w/p,refl,obs} = V_{in} [1 + \rho_{S>L} + \Gamma_{S>L} \rho_{pr} \Gamma_{L>S} + (\Gamma_{S>L} \rho_{L>S} \rho_{pr}^2 \Gamma_{L>S} + \Gamma_{S>L} \Gamma_{pr}^2 \Gamma_{L>S}) + 2\Gamma_{S>L} \rho_{pr} \Gamma_{pr}^2 \Gamma_{L>S} + \dots], \quad (9)$$

where

$$\rho_{pr} = \frac{\left(\frac{1}{Z_{pr}} + \frac{1}{Z_C}\right)^{-1} - Z_C}{\left(\frac{1}{Z_{pr}} + \frac{1}{Z_C}\right)^{-1} + Z_C} \quad (10)$$

and

$$\Gamma_{pr>L} = (1 - \rho_{pr}) \frac{Z_{pr}}{Z_{pr} + Z_C}, \quad (11)$$

where  $\Gamma_{pr>L}$  is the propagation coefficient at the probe/transmission line interface for the pulse continuing along the transmission line. Equation (11), for  $Z_{pr} = 50 \Omega$  and  $Z_C = 10 \Omega$ , gives  $\rho_{pr} = -0.091$  and  $\Gamma_{pr>L} = 0.909$ . The state levels for the first few reflections, where the first negative reflection has been arbitrarily selected to have a value of 0 V, are: 0.004, 0, 0.0373, and 0.030 V. The agreement between these values and those of the waveform are obscured by the roll-off characteristics of the transitions in the TDR waveform. However, these values are still in close agreement with those observed in Fig. 8 (solid line). The roll off in the tran-

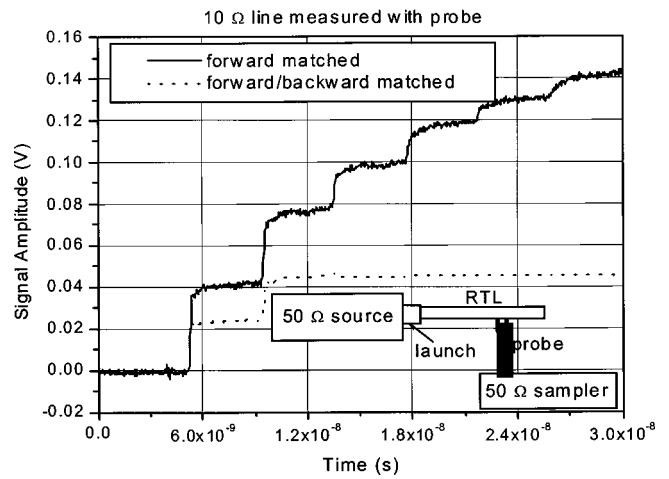


FIG. 9. The 10 Ω TDR of launch. The experimental arrangement is shown diagrammatically in the lower right.

sitions is probably affected by bandwidth of the probe contact resistors, as was the case for the launch resistors (see Sec. III B 2).

Similarly, the effect of the probe on the f/bd is assessed. The expected state levels for the TDR waveform are: 0.005, 0, 0.012, and 0.010 V (see Fig. 8, dotted line). Although the expected values for the TDR waveform levels are not the same as the waveform values, the agreement is close.

**4. 10 Ω TDR of launch end of test structure**

This section provides information on the magnitude of the backward-going signals that are reflected from the launch/TDR interface and that are subsequently measured by the 10 Ω TDR. These are signals that have passed through the interface and are reflecting between the open and TDR ends of the RTL. Ideally, these reflected signals should be eliminated to reduce errors in the computation of  $Z_C$ . Figure 9 shows the 10 Ω TDR of the launch for both the fd and f/bd. The experimental arrangement is shown diagrammatically in the lower right of Fig. 9. The state levels in these waveforms are described by

$$V_{refl,obs} = V_{in} \Gamma_{S>L} \Gamma_{pr>P} [1 + (\rho_{pr} \rho_{L>S} + \Gamma_{pr>L}) + (\Gamma_{pr>L}^2 \rho_{L>S} + \rho_{pr} \rho_{L>S} \Gamma_{pr>L} + \Gamma_{pr>L} \rho_{pr}) + \rho_{pr}^2 \rho_{L>S}^2 + \dots]. \quad (12)$$

For the fd, the expected values for the first three levels are: 0 V, 0.043 V, and 0.079 V. For the f/bd, the expected values for the first three levels are: 0, 0.024, and 0.044 V. These values are consistent, although not identical, with the first three waveform levels shown in Fig. 9.

**C. Probe design**

In this section, the design of the probe that will be used to extract the signals from the RTL is examined. The probe is one of the essential parts of this low-impedance TDR system. The design of the transmission line probe has several important considerations. The first consideration is that the probe has to have high enough bandwidth to support measurements of high-speed signals. To this end, we use the probe previ-

ously developed for high-bandwidth measurements on printed wiring boards.<sup>5</sup> The latest design of this probe has a 3 dB attenuation bandwidth of approximately 30 GHz. Another probe consideration is that it should have a sufficiently low enough impedance to allow a high measurement signal-to-noise ratio. Although the noise and the signal on the transmission line will be equally attenuated by the probe, the noise introduced into the waveform by the instrument is independent of probe impedance. Consequently, the probe should not attenuate the signal below the noise level introduced by the instrument. Another consideration is that the probe impedance be high enough so that it does not alter the propagating signal. These last two requirements are conflicting. However, since the input signal can typically be increased, the dominant consideration for the probe impedance will be to minimize signal perturbations. Equations (10) and (11) describe how the probe will affect signal propagation. Ideally, the reflection coefficient of the probe should be zero, but this requires that the impedance of the probe be infinite, which means for a passive probe that no signal is delivered to the instrument. The errors introduced by the probe come from the coupling of the propagating signal to the probe as the signal passes the probe and from reflections from the probe. The coupling of the signal to the probe can and should be calibrated. The probe reflection is caused by the lower impedance at the probe contact/RTL interface. Because of the probe, not all of the signal incident at the probe contact/RTL interface will pass by the probe and become incident on the reference/sample interface. The error in the calculated impedance caused by ignoring the probe can be described by

$$E_Z = \frac{(Z_{C,ideal} - Z_{C,actual})}{Z_{C,ideal}} = \left( \frac{1 + \rho_0}{1 - \rho_0} - \frac{1 + \Gamma_{pr > L\rho_0}}{1 - \Gamma_{pr > L\rho_0}} \right) \left( \frac{1 + \rho_0}{1 - \rho_0} \right)^{-1}, \quad (13)$$

where  $\rho_0$  is the reflection coefficient at the interface between the sample and the RTL. The results of Eq. (13), given as a percentage of  $Z_C$ , and as a function of  $\rho_0$ , are shown in Fig. 10. The different curves in Fig. 10 correspond to different ratios of probe impedance,  $Z_{pr}$  to  $Z_C$ .

An estimate for the largest acceptable amplitude perturbation,  $V_{lim}$ , in the TDR can also be determined. Using this estimated value for  $V_{lim}$  and the signal amplitude  $V_{in}$ , the lowest acceptable probe impedance can be determined. This limit can be computed by solving for Eq. (10) where  $\rho_{pr} = V_{lim}/V_{in}$

$$Z_{pr,lim} = \frac{1 - \frac{V_{lim}}{V_{in}}}{2 \frac{V_{lim}}{V_{in}}} Z_{TL}. \quad (14)$$

For example, for  $V_{in} = 0.25$  V,  $Z_C = 10$   $\Omega$ , and if the lowest acceptable perturbation in signal amplitude is 0.0025 V (1% of amplitude), then  $Z_{pr,lim} = 495$   $\Omega$ . For a 10  $\Omega$  line, the impedance ratio is in close agreement to the curve labeled "0.01" in Fig. 10. To achieve a high impedance probe, a resistor can be added in series to the probe, the results of

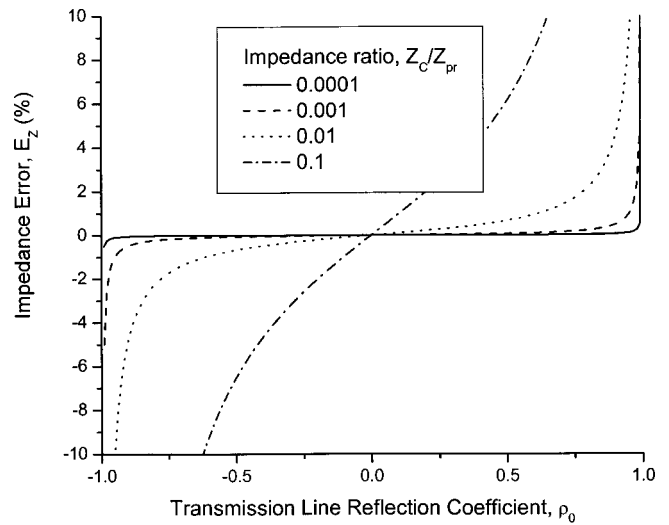


FIG. 10. Probe induced errors in the calculation of  $Z_C$  of the characteristic impedance of a sample transmission line.

which are shown in Fig. 11. The amplitude difference between the curves labeled "no probe" and "probe +475 ohm resistor" is due to scaling; the values used in the latter curve were scaled based on the dc measured resistance values of the probe contact resistor.

#### IV. TDR MEASUREMENTS OF IMPEDANCE DISCONTINUITY IN 10 $\Omega$ TEST STRUCTURE

In this section, the measurement of the impedance discontinuity going from a 10  $\Omega$  transmission line to a 9  $\Omega$  transmission line (10–9  $\Omega$  transition) is described and analyzed. It is assumed in this analysis that the 10  $\Omega$  line is accurately known and the 9  $\Omega$  line acts as the "unknown." The designs of both lines were based on simulations using a finite element field solver. Figure 12 shows the TDR waveform using a conventional 50  $\Omega$  TDR system. The characteristic impedance of the unknown line is calculated to be 8.85  $\Omega$ ; this is an error of about –1.6% relative to the 9  $\Omega$  line.

The same impedance discontinuity was measured using the low-impedance TDR system, as described in Fig. 3. This particular TDR used a 10  $\Omega$  transmission line as the test

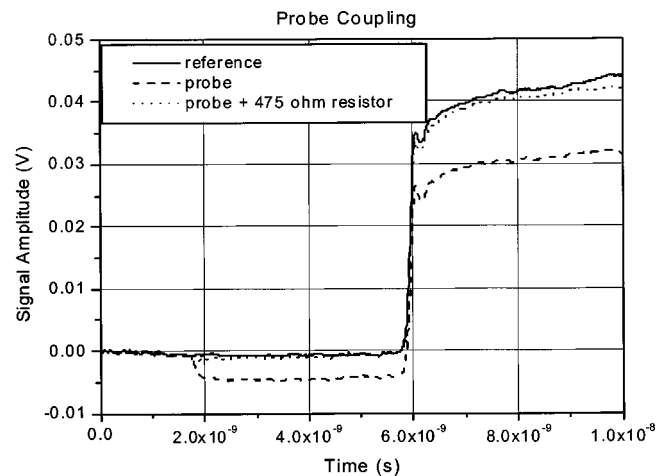


FIG. 11. TDR of probe with and without series resistor.

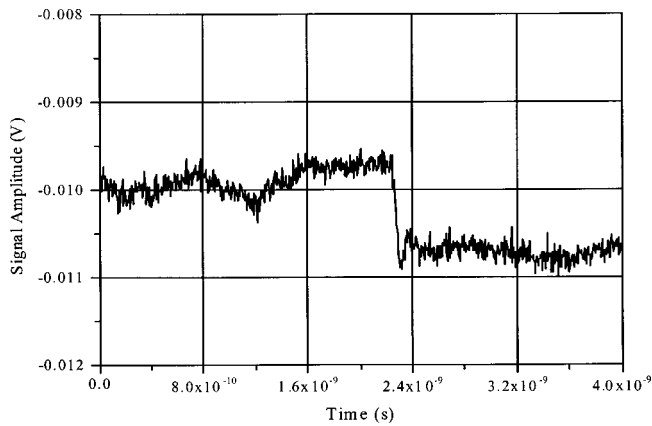


FIG. 12. TDR of 10  $\Omega$  to 9  $\Omega$  impedance discontinuity using conventional 50  $\Omega$  TDR system.

vehicle. The results of measurements using the 10  $\Omega$  TDR are shown in Fig. 13. The trace labeled “Reference open” was used to determine the location of the impedance discontinuity. The characteristic impedance of the unknown line is calculated to be 8.98  $\Omega$ ; this is an error of about  $-0.22\%$  relative to the 9  $\Omega$  line. This error is about seven times less than the error computed using the 50  $\Omega$  TDR. The difference in relative error between the 10 and 50  $\Omega$  TDRs may be due to the magnitude of the reflected signal (about 5.4 mV for the 10  $\Omega$  TDR system and about 0.9 mV for the 50  $\Omega$  TDR system) and/or the different settling of the TDR waveforms.

#### A. Measurement uncertainties and biases

Measurement uncertainties and biases will arise from several sources for the conventional TDR system. In conventional TDR, the calculation of the characteristic impedance of the unknown transmission line requires four state levels, two resistance values, and the characteristic impedance of the reference line,  $Z_{C,R}$ . In the low-impedance TDR described here, the calculation requires the values of three state levels and of  $Z_{C,R}$ . The state levels for the conventional TDR are the low and high states of the input and reflected steps. In the low-impedance TDR, the required state levels

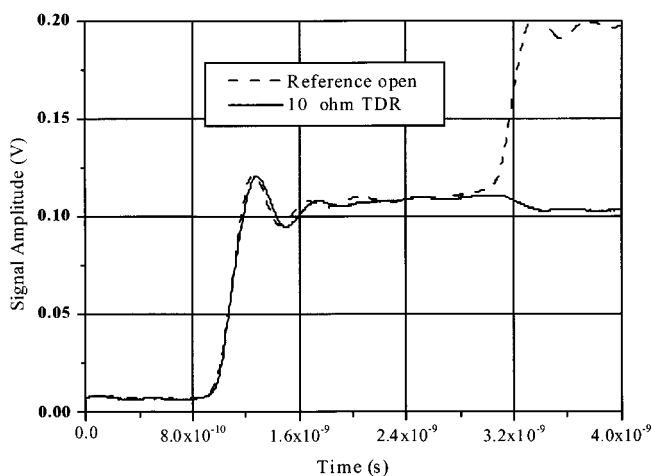


FIG. 13. TDR of 10  $\Omega$  to 9  $\Omega$  impedance discontinuity using 10  $\Omega$  TDR system. The trace labeled as Reference open was used to determine location of impedance discontinuity.

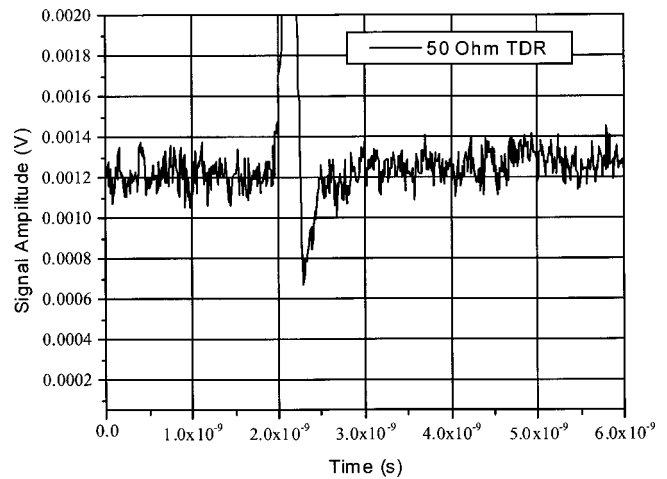


FIG. 14. TDR of 2  $\Omega$  to 2.2  $\Omega$  impedance discontinuity using conventional 50  $\Omega$  TDR system.

are the high and low states of the input step and the low or high state of the reflected step. The resistance values required in the conventional TDR are that of  $R_1$  and  $R_2$ , and are either supplied by a manufacturer or measured. The value of  $Z_{C,R}$  can be either measured or simulated, as was the case here. The values of the state levels are obtained from TDR measurements and are taken from regions of the TDR waveform that display nominally static levels. These regions may contain oscillations or have a nonzero slope. The values of state levels,  $R_1$ ,  $R_2$ , and  $Z_{C,R}$ , may be biased or have an offset error. This offset or bias will affect the value of the characteristic impedance of the unknown line,  $Z_{C,?}$ . The uncertainties in these values will contribute to uncertainties in  $Z_{C,?}$ .

#### V. TDR MEASUREMENTS OF IMPEDANCE DISCONTINUITY IN 2 $\Omega$ TEST STRUCTURE

Similar to what was done in Sec. IV, in this section the measurement of the impedance discontinuity going from a 2  $\Omega$  transmission line to a 2.2  $\Omega$  transmission line is described and analyzed. It is assumed that the 2  $\Omega$  line is ac-

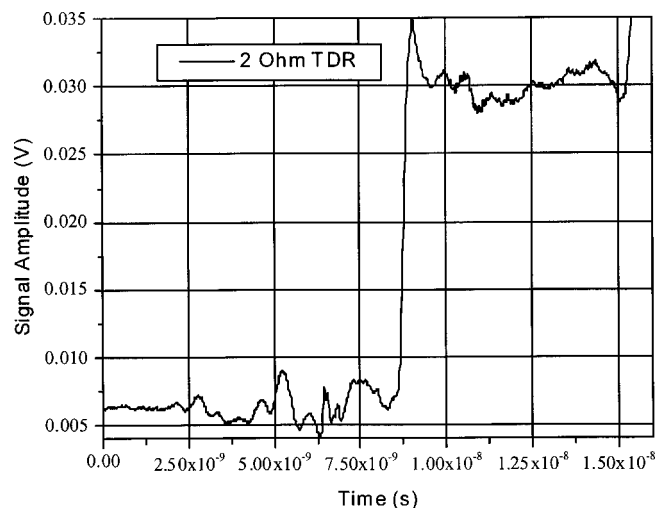


FIG. 15. TDR of 2  $\Omega$  to 2.2  $\Omega$  impedance discontinuity using 2  $\Omega$  TDR system.

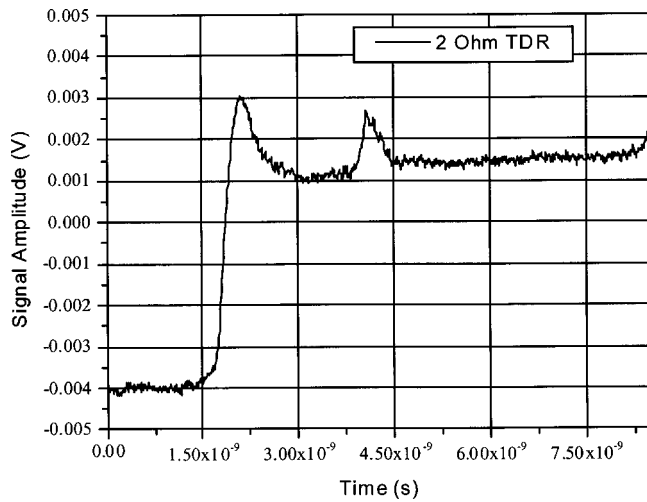


FIG. 16. TDR of 2  $\Omega$  to 2.2  $\Omega$  impedance discontinuity using 2  $\Omega$  TDR system. The pulse source was provided by the 50  $\Omega$  TDR system.

curately known and the 2.2  $\Omega$  line acts as the “unknown.” Figure 14 is the TDR waveform of this discontinuity using the 50  $\Omega$  TDR system. The transition between the 2  $\Omega$  and 2.2  $\Omega$  line occurs around 2 ns. The slight change in level around 4.5 ns is due to another impedance discontinuity. Al-

though it may be possible to estimate the characteristic impedance of the line attached to the 2  $\Omega$  reference line, it would be a very rough estimate (around 2.06  $\Omega$ ). Figure 15 is a TDR waveform of the discontinuity using the 2  $\Omega$  TDR. However, it is difficult to ascertain any levels for certain because of the oscillations at the state levels. These oscillations are an artifact of the “flat” pulse generator used. On the other hand, if the pulse from the 50  $\Omega$  TDR is used as the pulse, the waveform shown in Fig. 16 results. The input pulse starts around 1.8 ns, the reflection from the 2 to 2.2  $\Omega$  discontinuity occurs around 4.2 ns, and another reflection occurs around 6.6 ns. The nominally flat regions between these instants are used to compute the state levels, from which the reflection coefficient and then  $Z_{C,\gamma}$  are calculated. For this data,  $Z_{C,\gamma}$  is estimated to be around 2.24  $\Omega$ , which is an error of about 1.8% relative to the 2.2  $\Omega$  line.

<sup>1</sup>N. G. Paulter, IEEE Trans. Instrum. Meas. **50**, 1381 (2001).

<sup>2</sup>E. Zhong and T. A. Lipo, IEEE Trans. Ind. Appl. **31**, 1247 (1995).

<sup>3</sup>T. Guo, D. Y. Chen, and F. C. Lee, IEEE Trans. Power Elec. **11**, 480 (1996).

<sup>4</sup>H. Zhu, A. R. Hefner, Jr., and J.-S. Lai, IEEE Trans. Power Elec. **14**, 622 (1999).

<sup>5</sup>N. G. Paulter and R. H. Palm, Proceedings of the Technical Conference, IPC Printed Circuits Expo, Long Beach, CA, March 1999, p. S19-4-1.